

Article

Quantitative Evaluation of Municipal Wastewater Disinfection by 280 nm UVC LED

Linlong Yu ¹, Nicole Acosta ², Maria A. Bautista ³, Janine McCalder ³, Jode Himann ⁴, Samuel Pogosian ⁴, Casey R. J. Hubert ³, Michael D. Parkins ² and Gopal Achari ^{1,*}

¹ Department of Civil Engineering, University of Calgary, 2500 University Drive NW, Calgary, AB T2N 1N4, Canada

² Department of Microbiology, Immunology and Infectious Diseases, University of Calgary, 2500 University Drive NW, Calgary, AB T2N 1N4, Canada

³ Department of Biological Science, University of Calgary, 2500 University Drive NW, Calgary, AB T2N 1N4, Canada

⁴ Nermalux LED Lighting, 1018 72 Ave NE, Calgary, AB T2E 8V9, Canada

* Correspondence: gachari@ucalgary.ca

Abstract: UV-LED irradiation has attracted attention in water and wastewater disinfection applications. However, no studies have quantitatively investigated the impact of light intensity on the UV dosage for the same magnitude of disinfection. This study presents a powerful 280 nm UV-LED photoreactor with adjustable light intensity to disinfect municipal wastewater contaminated with *E. coli*, SARS-CoV-2 genetic materials and others. The disinfection performance of the 280 nm LED was also compared with 405 nm visible light LEDs, in terms of inactivating *E. coli* and total coliforms, as well as reducing cATP activities. The results showed that the UV dose needed per log reduction of *E. coli* and total coliforms, as well as cATP, could be decreased by increasing the light intensity within the investigated range (0–9640 $\mu\text{W}/\text{cm}^2$). Higher energy consumption is needed for microbial disinfection using the 405 nm LED when compared to 280 nm LED. The signal of SARS-CoV-2 genetic material in wastewater and the SARS-CoV-2 spike protein in pure water decreased upon 280 nm UV irradiation.

Keywords: LED; UVC; disinfection; SARS-CoV-2; *E. coli*; total coliform; cellular ATP



Citation: Yu, L.; Acosta, N.; Bautista, M.A.; McCalder, J.; Himann, J.; Pogosian, S.; Hubert, C.R.J.; Parkins, M.D.; Achari, G. Quantitative Evaluation of Municipal Wastewater Disinfection by 280 nm UVC LED.

Water **2023**, *15*, 1257. <https://doi.org/10.3390/w15071257>

Academic Editors: Gang Wen, Shiquan Sun and Zhengqian Liu

Received: 7 March 2023

Revised: 17 March 2023

Accepted: 20 March 2023

Published: 23 March 2023



Copyright: © 2023 by the authors. Licensee MDPI, Basel, Switzerland. This article is an open access article distributed under the terms and conditions of the Creative Commons Attribution (CC BY) license (<https://creativecommons.org/licenses/by/4.0/>).

1. Introduction

Ultraviolet (UV) irradiation is a known disinfectant that inactivates viruses, bacteria, protozoa and other pathogens in water and wastewater [1,2]. The UV irradiation disinfection technology utilizes mainly UVC irradiation (<280 nm), although UVB (280–315 nm) and UVA (315–400 nm) are also reported to inactivate pathogens, with less efficacy [2]. The genetic material of pathogens, consisting of DNA or RNA, can absorb UV radiation from 200 nm to 300 nm [3]. The absorption of UVC can lead to photo-dimeric lesions in DNA and RNA photo-byproducts, such as uracil dimers and RNA–protein cross-links, that can prevent their transcription and replication [2,4]. UVC irradiation in wastewater treatment plants is typically provided by mercury fluorescence lamps, which are fragile and contain mercury, a potential hazard to the environment and human health. These mercury lamps have wall plug efficiency ranging between 15% and 35%, and have a short lifetime (<10,000 h) [2]. In recent decades, a novel light source, the light-emitting diode (LED), has been developed to replace mercury fluorescent lamps for illumination. LEDs have many advantages over conventional light sources, including potentially less energy consumption, a longer lifetime, a narrow emission spectrum, improved robustness, a smaller size, faster switching, and a greater durability and reliability, in addition to being more environmentally friendly, due to not using mercury [5]. UVC-LED has been widely reported to successfully inactivate various pathogens in water, including *E. coli*, *P. aeruginosa*, *B. subtilis*,

MS2 bacteriophages, T7 bacteriophages and others [2,5–7]. Although UVC-LED is more expensive and has a lower wall plug efficiency than mercury lamps, its development is expected to follow a similar trajectory to visible LEDs [6].

The UV disinfection efficiency of *E. coli*, total coliforms and other bacteria is often evaluated by measuring the bacterial counts before and after UV irradiation. The bacteria counts can be estimated based on either colony-forming units (CFU) or most the probable number (MPN), measured through culture-based methods [7–10]. The culture-based methods usually take 18–24 h to incubate the water samples in selective media [7]. Recently, the cellular adenosine triphosphate (cATP) assay has attracted attention in monitoring the level of microorganisms and evaluating disinfection performance. The ATP molecule provides the major energy source for microbial metabolism and is considered a measure of cell viability [11]. During the ATP assay, the reaction between ATP molecules and a mixture of luciferin and luciferase can generate light. The relative light intensity of luminance is proportional to the concentration of ATP in a sample. Unlike culture-based methods, the cATP assay can be completed in minutes. The method is straightforward, and requires a relatively small amount of water for the measurement. However, it can not be used to distinguish between different microorganisms, and cannot quantify the exact amount of bacteria in the water. Although the UV dose for *E. coli* and total coliform disinfection has been widely reported, to the best of our knowledge, no research has quantitatively studied the impact of UVC-LED light intensity on the UV dose required for the same log reduction of *E. coli* and total coliforms during disinfection.

Since 2020, severe acute respiratory syndrome coronavirus 2 (SARS-CoV-2) RNA has been frequently detected in domestic wastewater through wastewater-based epidemiology (WBE) monitoring programs [12–16]. The SARS-CoV-2 RNA may be excreted from SARS-CoV-2-infected patients [17–21] and eventually makes its way into domestic wastewater treatment plants. Generally, the detection of SARS-CoV-2 genetic material in wastewater is not considered to pose a severe risk of infection, as its detection only requires the presence of genome fragments and not whole, intact viral particles [22]. In the past two years, researchers have investigated the reduction of the infectivity of SARS-CoV-2 using UVC irradiation [23–25]. The reported UV dose required to achieve one log reduction of SARS-CoV-2 varied from a few mJ/cm^2 to hundreds of mJ/cm^2 [23–25]. However, no study has focused on the impact of UVC irradiation on SARS-CoV-2 genetic materials in wastewater. There is a need to understand the impact of UVC LED irradiation on the reduction of the SARS-CoV-2 RNA signal, while achieving *E. coli* and total coliform disinfection in domestic wastewater.

In this study, we designed and fabricated a powerful intensity-adjustable UVC-LED (280 nm) reactor and developed a mathematical model to simulate its radiation field. The developed LED reactor was then tested in terms of its ability to inactivate fecal pathogens, such as *E. coli* and coliforms, in WWTP primary influent and secondary effluent. Both culture-based methods and the cATP assay were used to evaluate the disinfection efficiency. We have also quantified the effect of light intensity on the 280 nm UV dose required for inactivating *E. coli* and total coliforms. Furthermore, from an energy perspective, the 280 nm LED's disinfection performance was compared to that of the 405 nm LED. The effects of UVC-LED irradiation on the amount of SARS-CoV-2 genetic material and the SARS-CoV-2 spike protein in water were also investigated in this study.

2. Materials and Methods

2.1. Chemicals

BSA with 99% purity and Lysogeny Broth (Lennox, Richardson, TX, USA) were purchased from Sigma Aldrich, Oakville, ON, Canada; The SARS-CoV-2 Spike Protein (S-ECD) (aa14-1213) were obtained from Fisher Scientific. A Quench-Gone aqueous test kit (LuminUltra, Fredericton, NB, Canada) was purchased from Hach. Colilert reagents and test kits were purchased from IDEXX (Markham, ON, Canada). Sterile, distilled water was used to dilute the samples in this study, if necessary. The primary influent and secondary

effluent were collected from the Pine Creek wastewater treatment plant in Calgary, and stored at 4 °C until the UV irradiation experiments.

2.2. Design and Fabrication of LED Reactors

Two LED photo-reactors with top irradiation were designed and fabricated for this project. The first photoreactor was built with UVC LEDs (NCSU334B, Nichia Corporation), while the second one was built with near UV/blue LEDs (NVSU119C, Nichia Corporation). The specifications of both LEDs are provided in Table 1, and their relative emission spectra are shown in Figure 1. The NCSU334B LED has a peak emission wavelength at 280 nm, with a half-width of 10 nm, while NVSU119C has a peak emission wavelength at 405 nm, with a half-width of 12 nm.

Table 1. Specifications of LED (obtained from Nichia Corporation).

Item	NCSU334B	NVSU119C
Peak wavelength	280 nm	405 nm
Maximum radiant flux	100 mW	2840 mW
Spectrum half-width	10 nm	12 nm
Operating temperature	−10~85 °C	−10~85 °C
Maximum forward current	500 mA	1400 mA
Wall-Plug efficiency	65.4% *	3.6% *

Note: * The wall-plug efficiency was estimated as the optical power output divided by the electrical power input.

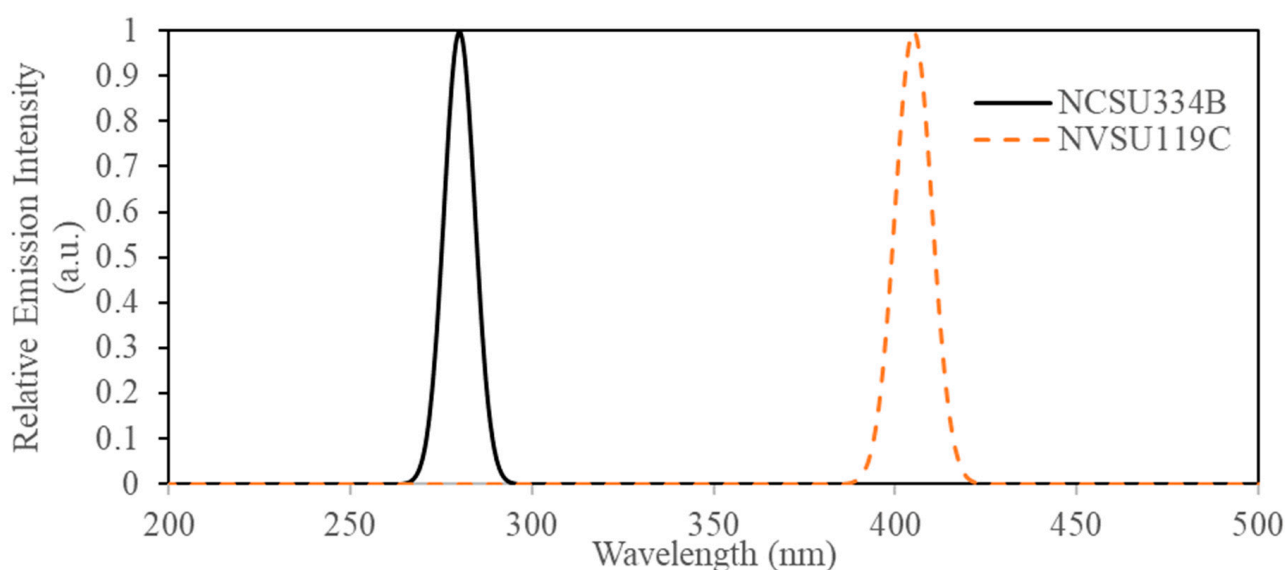


Figure 1. Relative emission intensity for NCSU334B and NVSU119C LEDs.

Both LED reactors have the same configuration, as shown in Figure 2. A 4 × 4 LED array was prepared and mounted on an aluminum plate. The distance between each adjacent LED was about 3 cm. Groups of four LEDs each were connected in series and powered by direct current (DC). The light intensity generated by the LED reactor could be controlled by adjusting the current (0~500 mA). Active cooling fans were used to avoid overheating during the LED reactor operation. The LED module was housed in a fiberglass-based enclosure, with dimensions of 30 cm (L) × 20 cm (W) × 40 cm (H). A lab jack was used to adjust the distance between the sample and LED array.

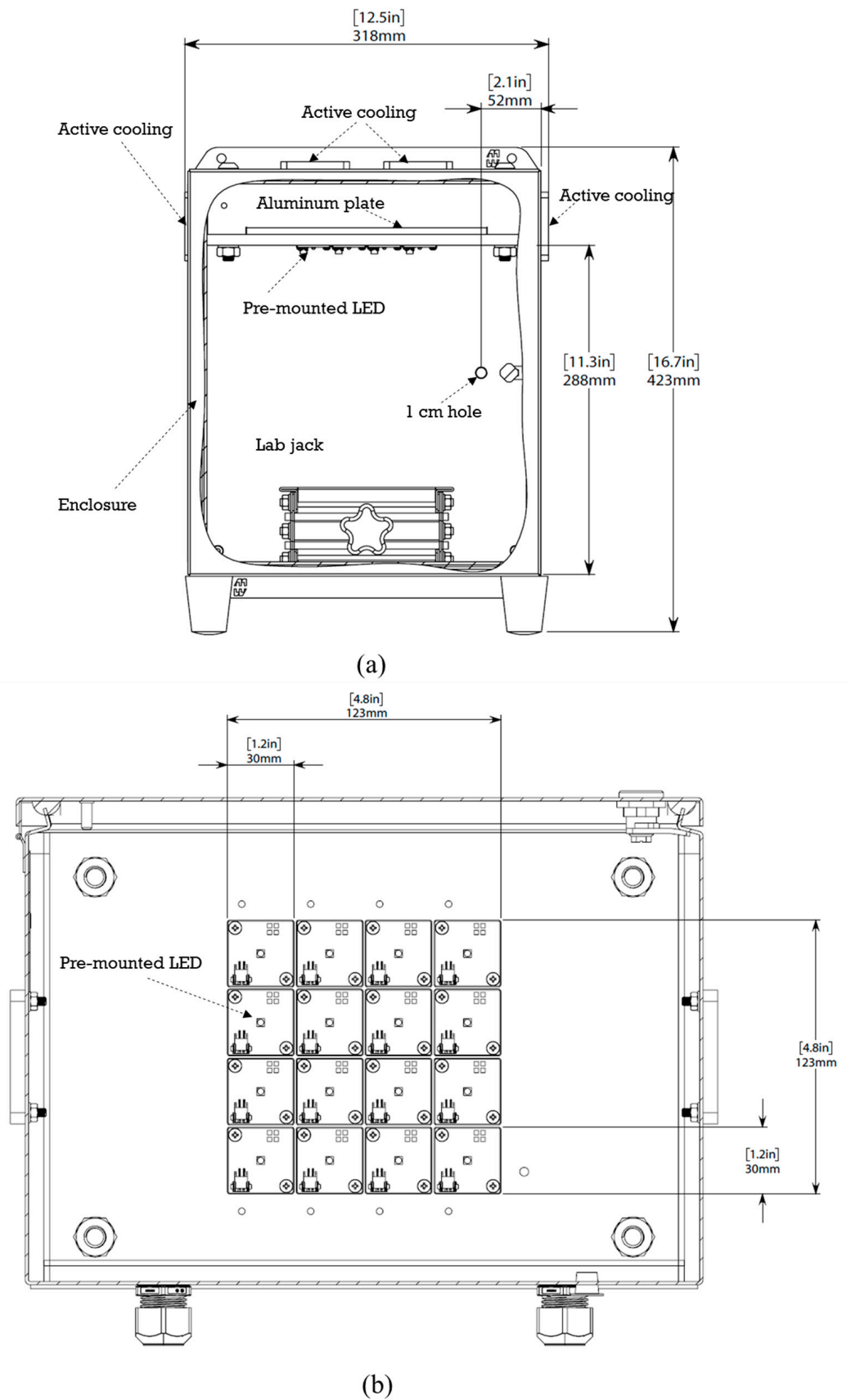


Figure 2. Schematics of LED photoreactor: (a) front view; (b) top view.

2.3. Disinfection Experiments Using UV LED Irradiation

Disinfection experiments were conducted in the 280 nm or 405 nm LED reactors. For each experiment, a sterile Petri dish beaker (diameter = 7.3 cm), containing 60 mL of WWTP primary influent or secondary effluent, was placed 5 cm from the LED array. A magnetic stirrer continuously mixed the water samples during irradiation. The depth of water in the beaker was around 1.3 cm. The light intensity of the LED photoreactor was controlled for by adjusting the direct current input (5–500 mA). All experiments were conducted in duplicates and the temperature of the water samples was brought to the room temperature (around 20 °C) before the disinfection experiments. The detailed experimental conditions, including the light intensities, the irradiation time, the water matrix and the biological parameters to be analyzed for each test, can be found in Supplementary Table S1.

Initially, the experiments were conducted on WWTP secondary effluent, in order to determine the UV dose–response relationships for cATP activity, as well as total coliform and *E. coli* levels. All cATP experiments were conducted on the unaltered WWTP secondary effluent. Five milliliter water samples were collected at different irradiation times for the cATP activity assay. For total coliform and *E. coli* experiments, one liter of WWTP secondary effluent was supplemented with 1 g of LB broth culture medium and incubated at 35 °C for 24 h, in order to boost its microbial population. The disinfection experiments were then conducted in the incubated WWTP secondary effluent at around 20 °C. Each 2 mL water sample was collected at different irradiation times for *E. coli* and total coliform analysis.

Further experiments were conducted on unaltered WWTP primary influent contaminated with SARS-CoV-2 RNA at around 20 °C. The effects of 280 nm LED irradiation on a variety of pathogens and biological signals present in the wastewater, including *E. coli*, total coliforms, cellular ATP, and the SARS-CoV-2 RNA genome, were evaluated. Every 60 mL WWTP primary influent sample was exposed to 280 nm LED irradiation with different light intensities for different durations. After irradiation, every 40 mL water sample was collected and kept in the sterilized 50 mL centrifuge tubes with 10 g of sodium chloride, for viral genomic RNA analysis. The rest of the irradiated sample was kept for the total coliform and *E. coli* analysis. Additional tests on SARS-CoV-2 spike protein and BSA levels in distilled water were also performed to shed additional light on the UV inactivation of SARS-CoV-2.

2.4. Chemical Analysis

2.4.1. BSA and SARS-CoV-2 Spike Protein Analysis

BSA and SARS-CoV-2 spike protein levels in water samples were measured using the Bradford protein assay [26]. An 0.8 mL water sample, or standard, was mixed with 0.2 mL of Bio-Rad Protein Assay Dye Reagent (#5000006, Bio-Rad Laboratories, Inc., Hercules, CA, USA), and kept at room temperature in the dark for 15 min. The absorbance of the mixture at 595 nm was measured in a micro cuvette with a 1 cm path length, with a Shimadzu UV-VIS spectrophotometer (UV-2600). The concentrations of BSA and SARS-CoV-2 spike protein were calculated based on the sample' absorbance at 595 nm and calibration curves prepared from standards.

2.4.2. cATP Analysis

The level of cATP in water samples was quantified by the Quench-Gone aqueous test kit (Hach, London, ON, Canada). Each 5 mL sample was passed through a 0.45 µm polytetrafluoroethylene (PTFE) filter. Then, 1 mL of UltraLyse 7 (a lysis solution) was slowly passed through the filter to dryness, and collected in a 9 mL UltraLute (a diluent) tube. The solution in the UltraLute tube was then mixed, and 0.1 mL of such solution was transferred to a 12 × 55 mm test tube. Then, 0.1 mL of Luminase containing the enzyme luciferase was added to the test tube. The bioluminescence intensity generated from the test tube was then measured on a luminometer. The cATP level was calculated based on the bioluminescence intensity of the samples and the standard.

2.4.3. Total Coliform and *E. coli* Analysis

Total coliform and *E. coli* levels in the water samples were quantified using Colilert test kits. Every 100 mL diluted water sample was mixed with Colilert reagent and poured into a 97-well Quanti-tray. The trays were then sealed and incubated at 35 ± 0.5 °C for 24 h. After incubation, the number of yellow wells that appeared on the 97-well Quanti-trays was counted and compared to the most probable number (MPN) table, in order to determine the concentration of total coliforms. The concentration of *E. coli* in the sample was determined by counting the number of fluorescent wells that appeared in the 97-well Quanti-tray under UVA irradiation.

2.4.4. SARS-CoV-2 Analysis

Wastewater samples were processed, and nucleic acids were extracted in the University of Calgary's Advancing Canadian Water Assets (ACWA) facility, by using an affinity column method (Whitney et al. [27] with modifications [12]). Each 40 mL water sample preserved with 10 g of sodium chloride was added with 400 µL of TE buffer and spiked with 200 µL of attenuated bovine coronavirus as a positive control. The mixture was then filtered with a 5 µm polyvinylidene difluoride (PVDF) membrane to remove the particles. The filtrate, containing SARS-CoV-2 RNA, was added to 40 mL of 70% ethanol and passed through a silica spin column (Zymo III-P silica spin column, Zymo Research). Then, 10 mL of 4S-WB1 buffer and 20 mL of 4S-WB2 buffer were passed through the column, in order to minimize downstream inhibition. In the end, nucleic acids bound to the silica column were then eluted using 150 µL of RNase-free water (50 °C) and stored immediately at -80 °C for RT-PCR analysis. Purified nucleic acids in RNase-free water were quantified by RT-PCR assays, targeting the N1 region of the nucleocapsid gene of SARS-CoV-2 virus.

3. Results and Discussions

3.1. Simulated Radiation Field for 405 nm and 280 nm LED Photoreactors

In this study, a 2-D radiation field for the designed LED reactor was simulated using Equation (1), modified from Yu et al. [28,29], and the average light intensity received by the testing Petri dish was calculated using Equation (2).

$$I(x, y, D) = \sum_{i=1}^m I_r * \text{Re}(\theta) * \frac{d_o^2 * D}{(D^2 + (x - x_i)^2 + (y - y_i)^2)^{3/2}} \quad (1)$$

$$I_a = \frac{\iint I(x, y, D) dA}{A} \quad (2)$$

As shown in Figure 3, D is the distance between the Petri dish and the LED panel, x and y are the coordinates of the point, in terms of the Petri dish plane, where the light intensity needs to be calculated; $I(x, y, D)$ is the light intensity at a coordinate of (x, y, D); θ is the view angle, which is equal to $\arctan\left(\frac{\sqrt{(x-x_i)^2+(y-y_i)^2}}{D}\right)$; I_r is the reference light intensity for each LED lamp with a zero view angle and a reference distance (d_o); x_i and y_i are the coordinates for *i*th LED lamp; *m* is the number of LED lamps; $\text{Re}(\theta)$ is the radiation directivity function for the LED lamp, which is defined as the ratio between light intensity with a view angle θ and the light intensity with a view angle of zero at the same distance from the light source; *A* is the area of the Petri dish.

The radiation directivity function ($\text{Re}(\theta)$) for the LED lamp was developed, based on the relative radiant intensity data extracted from the manufacturer's specifications (NVSU119C and NCSU334B). The developed radiation directivity functions for the 280 nm LED (NCSU334B) and 405 nm LED (NVSU119C) can be seen in Equations (3) and (4), respectively:

$$\text{Re}_{280nm}(\theta) = \begin{cases} 1 + 0.2067 * \theta^2 + 0.128 * \theta & ; 0 \leq \theta < 0.4363 \\ 1.1176 - 0.5089 * \theta^4 & ; 0.4363 \leq \theta \leq 1.22 \\ 0 & ; \theta > 1.22 \end{cases} \quad (3)$$

$$Re_{405nm}(\theta) = \begin{cases} 1 - 0.164 * \theta^2 & ; 0 \leq \theta < 0.96 \\ 1.3585 - 0.5509 * \theta^2 & ; 0.96 \leq \theta \leq 1.57 \\ 0 & ; \theta > 1.57 \end{cases} \quad (4)$$

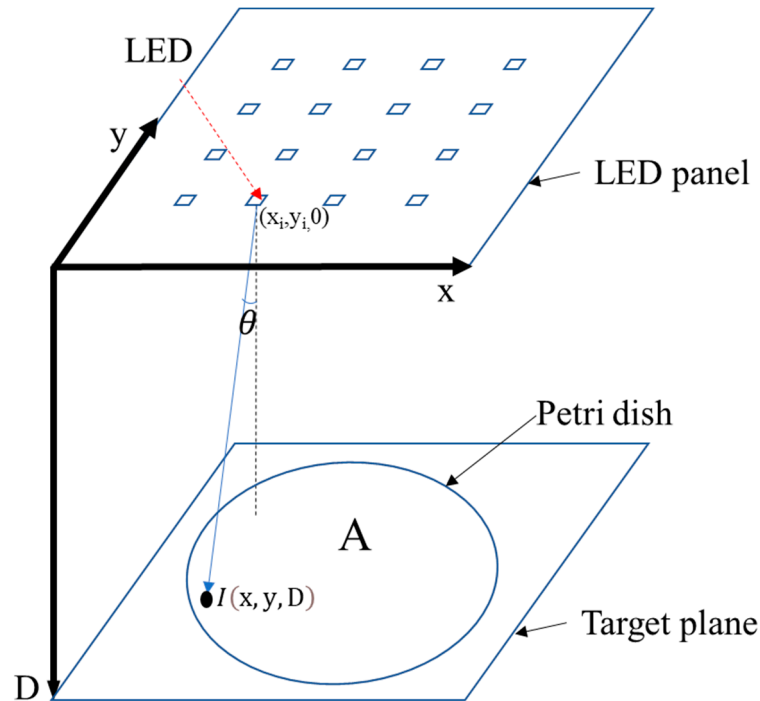


Figure 3. A schematic of the LED array and target plane for the radiation field model development.

In this study, the light intensity with a zero view angle and a distance of 10 cm was defined as a reference light intensity for Equation (1). The reference light intensities for 280 nm and 405 nm LEDs were measured by a PM100D radiometer (Thorlabs, Canada ULC Saint-Laurent, Montpellier, QC, Canada). When the input current for the LEDs was 500 mA, the reference light intensities for 280 nm and 405 nm LED were 0.373 mW/cm² and 4.57 mW/cm², respectively.

The 2D radiation fields with two different “D” values (1 cm and 5 cm), for both 280 nm and 405 nm LED reactors, are shown in Figure 4. The statistics of the light intensity distribution within the testing Petri dish are summarized in Table 2. The radiation field with a larger D is more homogenous. For the 280 nm LED reactor, when D is 5 cm, the average light intensity is 9.64 mW/cm², with a standard deviation of 0.44. In contrast, the average light intensity when D = 1 cm is 13.16 mW/cm², with a standard deviation of 8.2. The light intensity generated from the 405 nm LED was almost ten times higher than that generated from the 280 nm LED when the input current was the same. The reactor with homogenous light distribution would avoid the disinfection dead spots; therefore, D was set to 5 cm for the disinfection study. The UV dose in this study was calculated by multiplying the average light intensity received by the Petri dish with the irradiation time.

Table 2. Statistics of light intensity (mW/cm²), as received by the Petri dish.

Parameter	280 nm, 500 mA		405 nm, 500 mA	
	D = 1 cm	D = 5 cm	D = 1 cm	D = 5 cm
Mean	12.09	9.64	191	112
Standard deviation	8.51	0.48	85.5	5.12
Max	37.62	10.63	497	121
Minimum	3.32	8.74	102	102

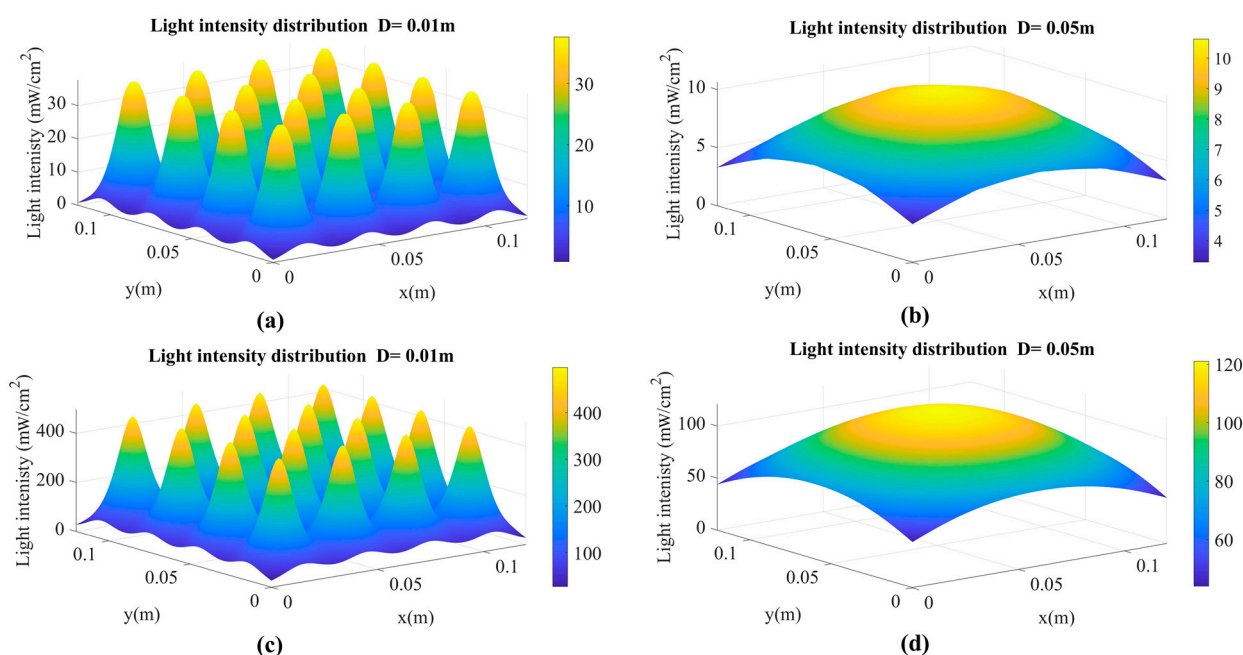


Figure 4. Light intensity distribution for the 280 nm LED reactor and 405 nm LED reactor (input current = 500 mA): (a) 280 nm LED reactor, $D = 0.01$ m; (b) 280 nm LED reactor, $D = 0.05$ m; (c) 405 nm LED reactor, $D = 0.01$ m; (d) 405 nm LED reactor, $D = 0.05$ m.

3.2. Effect of 280 nm UV-LED Irradiation on the *E. coli*, Total Coliform and cATP Levels in WWTP Secondary Effluent

In this study, the disinfection efficacy of a monochromatic 280 nm LED was evaluated by measuring the change in cATP, total coliform and *E. coli* levels in secondary WWTP secondary effluent samples, before and after irradiation. The UV dose is a key design parameter for UV-based water disinfection systems. Therefore, the log reductions of cATP, total coliform and *E. coli* levels versus UV dose at different UV light intensities are presented in Figure 5. As seen in Figure 5, the levels of cATP, *E. coli* and total coliform decreased significantly as the UV dose increased. After exposure to a 20 mJ/cm² UV dose, a 1~1.7 log reduction of total coliform and *E. coli* levels was observed, whereas less than one log reduction of cATP activity was observed with a much higher UV exposure of >2000 mJ/cm². These results show that the impact of 280 nm UV-LED irradiation on the ability to culture particular coliforms is much more significant than its impact on overall microbial activity. The absorption of 280 nm UV photons can cause the formation of dimers in genetic materials such as DNA and RNA, inhibiting the transcription and replication of genes from cells, as well as a loss of their ability to be cultured [6]. UV irradiation can slightly damage the membrane permeability, leading to a mild decay in cATP activity [8]. Several researchers have recently studied the impact of UV irradiation on cATP levels and concluded that a UV dose of less than 100 mJ/cm² is ineffective in degrading cATP [8,30,31]. Xu et al. [8] observed a reduction in cATP levels of 8.56% after exposure to a 100 mJ/cm² UV dose. Linklater and Örmeci [30] found that an 80 mJ/cm² UV dose did not cause a consistent increase or decrease in the cATP level in the water samples. Yang et al. [31] observed approximately 20% cATP reduction in *E. coli* and *S. aureus* samples with an 80 mJ/cm² UV dose. Our study showed that a UV dose more than 100 times this level is required to achieve the same log reduction of cATP as for cell numbers of *E. coli* and total coliform, indicating that the primary UV bacterial disinfection mechanism may depend on damaging the genetic material of these bacteria.

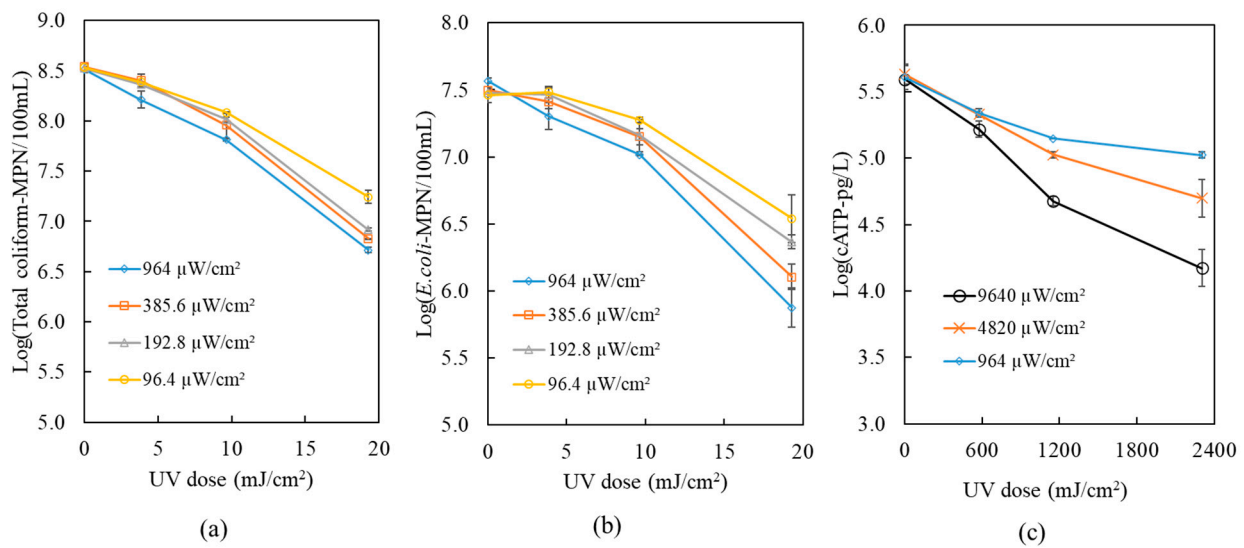


Figure 5. Disinfection of secondary wastewater effluent by a 280 nm LED: (a) total coliform log reduction, (b) *E. coli* log reduction and (c) cATP reduction.

The UV dose per log reduction values of cATP, total coliforms and *E. coli* were estimated using Equation (5), and the results are summarized in Table 3.

$$UV_{1-\log} = \frac{I_a \times t}{\log\left(\frac{N}{N_0}\right)} \tag{5}$$

where $UV_{1-\log}$ is the UV dose required for one log reduction of the microbiological parameter (mJ/cm^2); N_0 is the initial concentration of *E. coli* (MPN/100 mL), total coliforms (MPN/100 mL) or cATP (pg/L); N is the concentration of *E. coli* (MPN/100 mL), total coliforms (MPN/100 mL) or cATP (pg/L) after exposure to UV; I_a is the average light intensity (mW/cm^2); t is the irradiation time(s).

Table 3. Summary of the UV dose required for one log reduction of different parameters.

Parameter	Light Intensity ($\mu W/cm^2$)	$UV_{1-\log}$ (mJ/cm^2)
<i>E. coli</i>	96.4	17.97
	192.8	15.60
	385.6	12.62
	964	11.06
Total Coliform	96.4	14.35
	192.8	11.37
	385.6	10.61
	964	10.58
cATP	964	3654
	4820	2420
	9640	1562

As seen in Table 3, the UV intensity investigated for *E. coli* and total coliform disinfection varied from $96.4 \mu W/cm^2$ to $964 \mu W/cm^2$, while the UV intensity explored in the cATP experiment varied from $964 \mu W/cm^2$ to $9640 \mu W/cm^2$. The $UV_{1-\log}$ value of *E. coli* decreased from $18.64 mJ/cm^2$ to $11.47 mJ/cm^2$ when the UV intensity increased from $96 \mu W/cm^2$ to $964 \mu W/cm^2$. Similar trends were observed for the total coliform and cATP studies. These results suggested that the UV dose necessary for disinfection can be reduced by increasing the light intensity. Most publications have suggested first-order kinetics for UV disinfection, as shown in Equation (6). It is noted that the damage caused

by UV irradiation might be repaired through the nucleotide excision repair mechanism [32]. If the repair process is assumed to follow first-order kinetics as shown in Equation (7), then the observed disinfection kinetics by UV irradiation can be described using Equation (8).

$$\frac{N}{N_0} = e^{(-k_1 I t)} \quad (6)$$

$$\frac{N}{N_0} = e^{(K_2 t)} \quad (7)$$

$$\frac{N}{N_0} = e^{(-k_1 I + K_2) t} \quad (8)$$

where k_1 is the UV disinfection rate constant ($\text{cm}^2 \text{mW}^{-1} \text{s}^{-1}$), and K_2 is the repair kinetics rate constant (s^{-1}).

Substituting Equation (8) into Equation (5), $UV_{1-\log}$ can then be expressed as Equation (9). According to Equation (9), $UV_{1-\log}$ would decrease if the light intensity increased.

$$UV_{1-\log} = \frac{2.303}{(k_1 - K_2/I)} \quad (9)$$

3.3. Comparison of the 280 nm LED's and 405 nm LED's Disinfection Performance from an Energy Perspective

The blue LED (e.g., 405 nm) is a much more mature technology than the UVC (e.g., 280 nm) LED, having a higher wall plug efficiency, more powerful optical output, and more economical. Therefore, the disinfection capacity of the 405 nm LED was also investigated in this study and compared with the 280 nm LED. The results of disinfecting WWTP secondary effluent by the 405 nm LED are shown in Figure 6. Approximately, a 0.56 log reduction of *E. coli*, a 0.19 log reduction of total coliforms and a 0.31 log reduction of cATP were observed, with an irradiation dose of 202 J/cm^2 . The $UV_{1-\log}$ value and electrical energy required for a one log reduction in microbial inactivation ($EE_{1-\log}$) for 405 nm LED and 280 nm LED were calculated and summarized in Table 4. The $UV_{1-\log}$ values for *E. coli*, total coliforms and cATP, as measured by the 405 nm LED, were estimated to be 344, 1064 and 399 J/cm^2 , respectively, which are four orders, five orders, and two orders of magnitude higher than the values measured for the 280 nm LED reactor. The wall plug efficiency for the 405 nm LED is much larger better than that of the 280 nm, as shown in Table 1. Therefore, the difference in $EE_{1-\log}$ between the 280 nm LED and 405 nm LED is smaller than the difference in $UV_{1-\log}$ between the 280 nm LED and 405 nm LED. The $EE_{1-\log}$ values of *E. coli*, total coliforms and cATP, as measured for the 405 nm LED, were estimated to be 0.526×10^6 , 1.626×10^6 , and $0.610 \times 10^6 \text{ mJ/cm}^2$, respectively, which are three orders, three orders, and one order of magnitude higher than the values measured for the 280 nm LED reactor. Therefore, it seems that the use of the 405 nm LED for disinfection is inefficient from an energy consumption perspective. The disinfection mechanism for the 405 nm LED differs from 280 nm LED, as the nucleic acid's light absorption at 405 nm is much weaker than its absorption at 280 nm. Our results showed that the impact of the 405 nm LED on the number of coliforms and *E. coli* is similar to its effects on overall microbial metabolic activity, which was not the case for the 280 nm LED, as reported in Section 3.2. Even though the blue light disinfection mechanism is not fully understood, it is suggested that some endogenous molecules, such as iron-free porphyrins or flavins, can behave as photosensitizers [33]. Those photosensitizers might absorb the blue light and create cytotoxic reactive oxygen species (ROS).

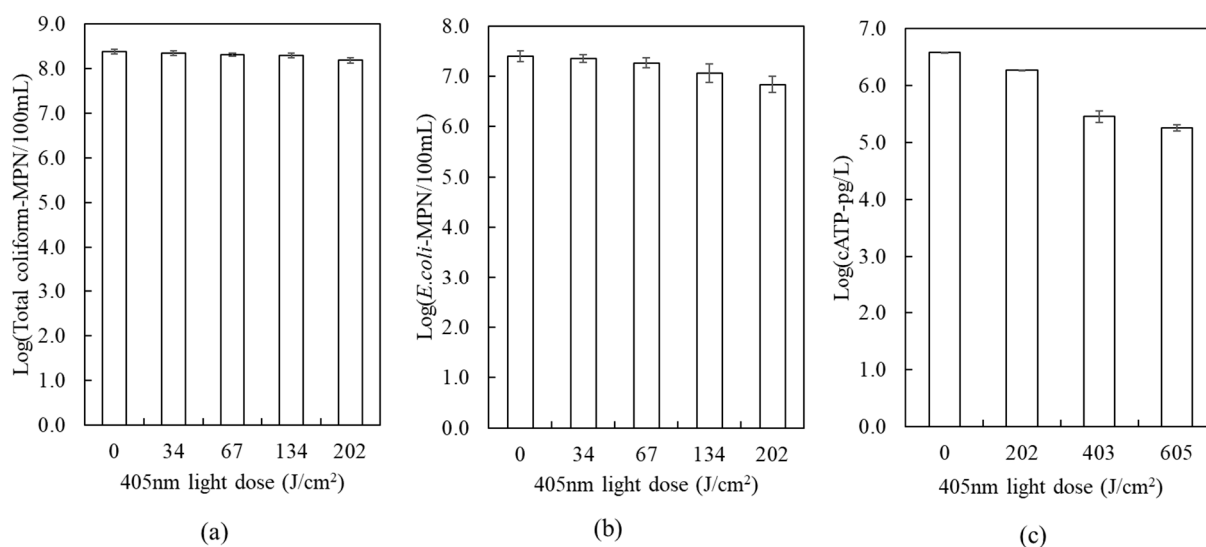


Figure 6. Disinfection of secondary wastewater effluent by the 405 nm LED: (a) total coliform log reduction, (b) *E. coli* log reduction, (c) cATP log reduction.

Table 4. Comparison of the 280 nm and 405 nm LEDs from an energy perspective.

Parameter	405 nm LED Reactor		280 nm LED Reactor	
	UV _{1-log} (mJ/cm ²)	EE _{1-log} (mJ/cm ²)	UV _{1-log} (mJ/cm ²)	EE _{1-log} (mJ/cm ²)
<i>E. coli</i>	344,534	526,506	11.06~17.97	304~494
Total coliform	1,064,285	1,626,406	10.58~14.35	291~394
cATP activity	399,715	610,831	1562~3654	42,976~66,577

3.4. The Impact of 280 nm LED Irradiation on SARS-CoV-2 RNA in WWTP Primary Influent

The focus of this section is to understand the impact of 280 nm LED irradiation on the SARS-CoV-2 genetic signal level in the WWTP primary influent. As a comparison, the inactivation of *E. coli* and total coliforms in the same WWTP primary influent sample was also quantified.

Figure 7 shows, approximately, a three log reduction of *E. coli* and total coliforms, as observed in the WWTP primary influent with a UV dose of 38.6 mJ/cm², similar to the disinfection results for the WWTP secondary effluent. However, the expression of the SARS-CoV-2 N1 gene in WWTP primary influent did not significantly decrease with a UV dose of 38.6 mJ/cm² and a light intensity of 96.4 μW/cm². A higher SARS-CoV-2 N1 reduction percentage (46%) was observed with a UV dose of 38.6 mJ/cm², when the light intensity was increased by ten-fold. At a light intensity of 9640 μW/cm², a 55% reduction of the SARS-CoV-2 N1 signal was noted with a UV dose of 96.4 mJ/cm², while 69% of SARS-CoV-2 N1 signal was lost from the water in which a UV dose of 578.4 mJ/cm² was applied. The impact of light intensity on the UV_{1-log} values, in terms of the degradation of SARS-CoV-2 N1, is inconclusive in the study due to insufficient data.

The same type of Nichia 280 nm LED has been reported to inactivate the live SARS-CoV-2 and recorded a four log reduction in SARS-CoV-2 infection viral titer with a UV dose of 51 mJ/cm² [34]. Biasin et al. [35] evaluated the infectivity of a UVC-irradiated SARS-CoV-2 virus in VeroE6 cells, and found that UVC irradiation at a dose of 3.7 mJ/cm²–84.4 mJ/cm² is highly effective in inactivating SARS-CoV-2 replication for both N1 and N2 copies. The degradation of SARS-CoV-2 genetic material in the present study is much lower than the published inactivation rate of the infectious SARS-CoV-2 [23–25]. The low degradation rate of SARS-CoV-2 genetic materials by UVC in WWTP primary influent is mainly due to its biological and biophysical properties of wastewater. The majority of SARS-CoV-2 genetic materials detected in the wastewater are fragments of SARS-CoV-2 RNA and are

noncontagious [36]. In addition, they have a large partition into the solid fraction over the liquid fraction in the primary influent [37,38]. Therefore, SARS-CoV-2 genetic materials are bound to the solids in the wastewater samples, making it difficult for UV photons to penetrate the solids and to degrade the SARS-CoV-2 genetic materials. The reduction of the SARS-CoV-2 N1 signal cannot be directly used to interpret the actual inactivation of the SARS-CoV-2 in the wastewater. Nonetheless, the SARS-CoV-2 N1 reduction results indicate that the 280 nm UVC LED can act on SARS-CoV-2 genetic materials, leading to SARS-CoV-2 inactivation. Therefore, the 280 nm LED can be used to manage wastewater contaminated with SARS-CoV-2 and other fecal pathogens.

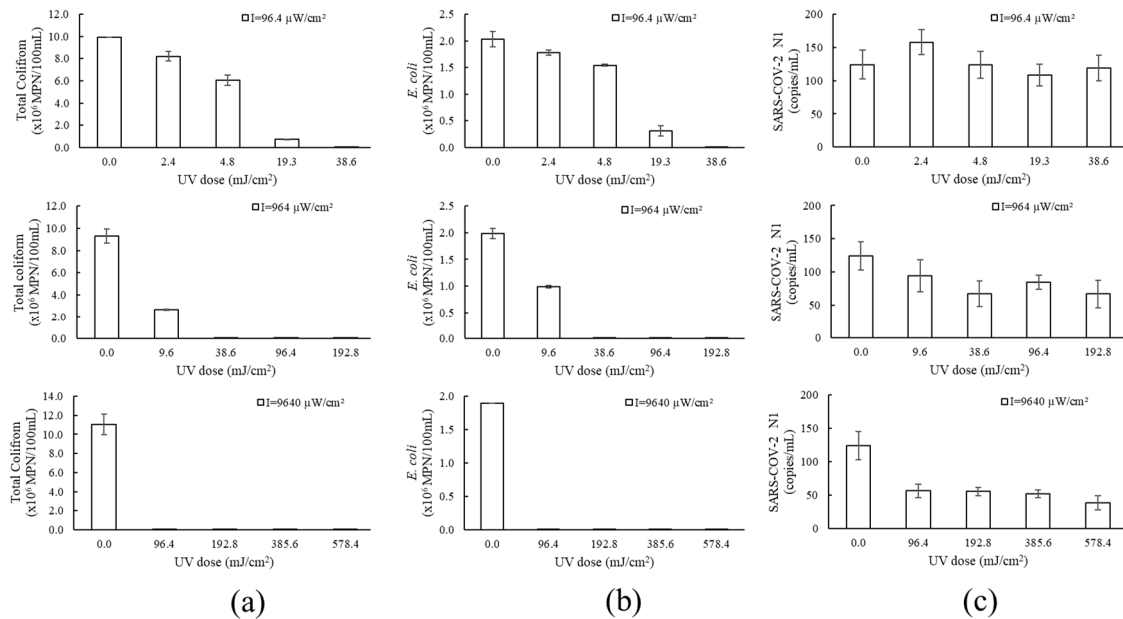


Figure 7. Disinfection of WWTP primary influent by 280 nm LED irradiation: (a) total coliform, (b) *E. coli* and (c) SARS-CoV-2 N1 levels.

3.5. The Impact of 280 nm LED Irradiation on BSA/Coronavirus Spike Protein

The impact of 280 nm LED irradiation on BSA and SARS-CoV-2 spike protein concentrations in deionized water is presented in Figure 8. Approximately, a 16% reduction of BSA or SARS-CoV-2 spike protein was observed with a UV dose of 52,056 mJ/cm². This result confirms that UV photons with a wavelength of 280 nm can attack the bacterial or viral protein, leading to the inactivation of the microorganism. The SARS-CoV-2 spike protein has a size of 1273 amino acids, which consists of a signal peptide (1–13 residues), S1 subunit (14–685 residues) and the S2 subunit (686–1273 residues) [39]. The SARS-CoV-2 spike protein (S-ECD) (aa14–1213) studied in this project contains 14–1213 residues. BSA is a single chain protein, containing 583 amino acids [40]. Both proteins contain aromatic amino acids, such as tyrosine and phenylalanine, with strong light absorption at 280 nm. The absorption of 280 nm photons by the aromatic amino acids might lead to the generation of radicals through hydrogen abstraction or hydrogen addition, causing photodegradation of proteins [41,42]. However, Lo et al. [43] reported insignificant differences in the SARS-CoV-2 spike protein and nucleocapsid (N) proteins between the control sample and the sample treated with 15 mJ/cm² of UV (254 nm). This could be due to the UV dose studied by Lo et al. [43] being thousands of times smaller than the one used in our study. If the photodegradation of SARS-CoV-2 N1 and SARS-CoV-2 spike protein is assumed to follow first order kinetics, the calculated $UV_{1-\log}$ for the degradation of the SARS-CoV-2 spike protein would be three orders of magnitude larger than the one predicted to degrade SARS-CoV-2 N1. This result reveals that the photodegradation of the SARS-CoV-2 spike protein cannot be the dominant mechanism for SARS-CoV-2 inactivation by UV irradiation.

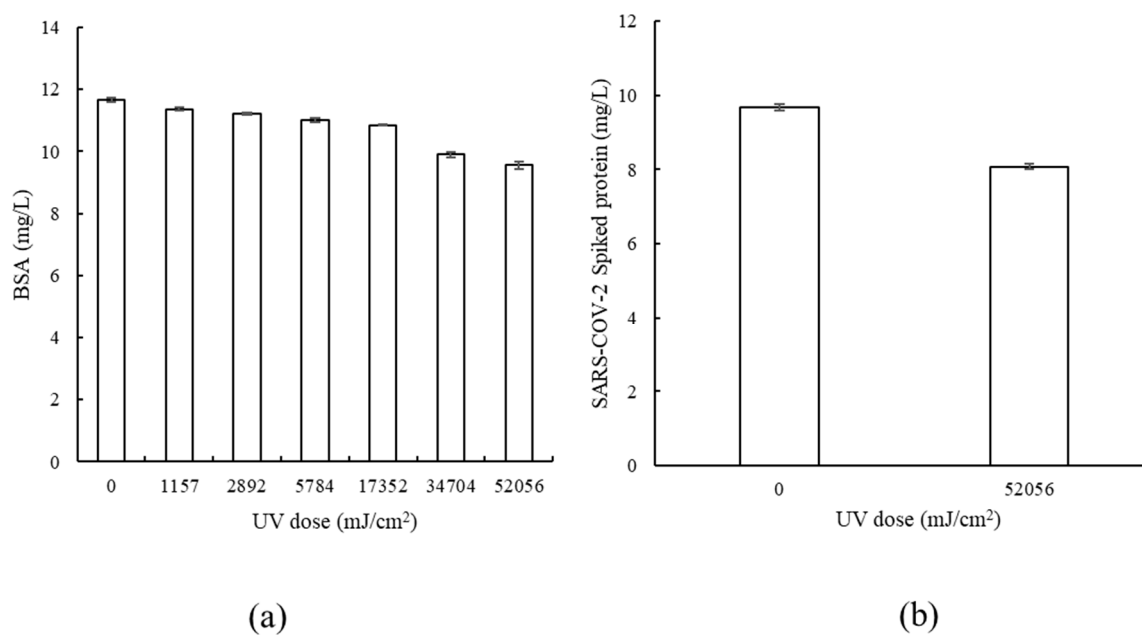


Figure 8. The impact of 280 nm LED irradiation (9640 $\mu\text{W}/\text{cm}^2$) on protein concentrations in wastewater: (a) BSA, (b) SARS-CoV-2 spike protein.

4. Conclusions

In this study, a 280 nm LED reactor and a 405 nm LED reactor with adjustable light intensity were designed and fabricated, in order to disinfect WWTP primary influent and secondary effluent. Both LED reactors are capable of inactivating *E. coli*, total coliforms and reducing cATP in WWTP secondary effluent. The 405 nm LED consumed a much higher amount of electrical energy than the 280 nm LED reactor in order to achieve the same log reduction of *E. coli* and total coliforms. The impact of the 280 nm LED on viable coliform bacteria is more significant than its impact on overall metabolic activity. Our results show that increasing the light intensity of UVC LED can reduce the energy required for water and wastewater disinfection. The 280 nm LED reduces the SARS-CoV-2 RNA signal in the wastewater at a rate much lower than the reported SARS-CoV-2 inactivation rate by UV irradiation. Considering the partitioning of the SARS-CoV-2 RNA in the solids of the wastewater treatment system and the biological properties of the SARS-CoV2 genetic material, we conclude it is inappropriate to use the SARS-CoV-2 RNA signal to interpret the inactivation of SARS-CoV-2 in the wastewater treatment system.

Supplementary Materials: The following supporting information can be downloaded at: <https://www.mdpi.com/article/10.3390/w15071257/s1>, Table S1: Detailed experimental condition.

Author Contributions: Conceptualization, L.Y., J.H., S.P. and G.A.; methodology, L.Y., N.A., M.A.B., J.M., C.R.J.H. and G.A.; formal analysis, L.Y.; investigation, L.Y., N.A., M.A.B. and J.M.; writing—original draft preparation, L.Y.; writing—review and editing, N.A., M.A.B., J.H., S.P., C.R.J.H., M.D.P. and G.A.; supervision, G.A.; project administration, G.A.; funding acquisition, G.A. All authors have read and agreed to the published version of the manuscript.

Funding: This research was funded by “Natural Sciences and Engineering Research Council of Canada (NSERC), grant number 10029430” and “The APC was funded by NSERC”.

Data Availability Statement: Not applicable.

Acknowledgments: We thank Advancing Canadian Water Assets for providing the WWTP primary influent and secondary effluent, and Nemalux for fabricating the LED photoreactors. We also thank Nichia for providing NCSU334B LED.

Conflicts of Interest: The authors declare no conflict of interest.

References

1. Augsburger, N.; Rachmadi, A.T.; Zaouri, N.; Lee, Y.; Hong, P.-Y. Recent Update on UV Disinfection to Fulfill the Disinfection Credit Value for Enteric Viruses in Water. *Environ. Sci. Technol.* **2021**, *55*, 16283–16298. [[CrossRef](#)] [[PubMed](#)]
2. Song, K.; Mohseni, M.; Taghipour, F. Application of Ultraviolet Light-Emitting Diodes (UV-LEDs) for Water Disinfection: A Review. *Water Res.* **2016**, *94*, 341–349. [[CrossRef](#)] [[PubMed](#)]
3. Görner, H. New Trends in Photobiology: Photochemistry of DNA and Related Biomolecules: Quantum Yields and Consequences of Photoionization. *J. Photochem. Photobiol. B Biol.* **1994**, *26*, 117–139. [[CrossRef](#)] [[PubMed](#)]
4. Beck, S.E.; Rodriguez, R.A.; Hawkins, M.A.; Hargy, T.M.; Larason, T.C.; Linden, K.G. Comparison of UV-Induced Inactivation and RNA Damage in MS2 Phage across the Germicidal UV Spectrum. *Appl. Environ. Microbiol.* **2016**, *82*, 1468–1474. [[CrossRef](#)]
5. Würtele, M.A.; Kolbe, T.; Lipsz, M.; Külberg, A.; Weyers, M.; Kneissl, M.; Jekel, M. Application of GaN-Based Ultraviolet-C Light Emitting Diodes—UV LEDs—For Water Disinfection. *Water Res.* **2011**, *45*, 1481–1489. [[CrossRef](#)]
6. Chen, J.; Loeb, S.; Kim, J.-H. LED Revolution: Fundamentals and Prospects for UV Disinfection Applications. *Environ. Sci. Water Res. Technol.* **2017**, *3*, 188–202. [[CrossRef](#)]
7. Li, G.-Q.; Wang, W.-L.; Huo, Z.-Y.; Lu, Y.; Hu, H.-Y. Comparison of UV-LED and Low Pressure UV for Water Disinfection: Photoreactivation and Dark Repair of *Escherichia coli*. *Water Res.* **2017**, *126*, 134–143. [[CrossRef](#)]
8. Xu, L.; Zhang, C.; Xu, P.; Wang, X.C. Mechanisms of Ultraviolet Disinfection and Chlorination of *Escherichia coli*: Culturability, Membrane Permeability, Metabolism, and Genetic Damage. *J. Environ. Sci.* **2018**, *65*, 356–366. [[CrossRef](#)]
9. Kollu, K.; Örmeci, B. Effect of Particles and Biofloculation on Ultraviolet Disinfection of *Escherichia coli*. *Water Res.* **2012**, *46*, 750–760. [[CrossRef](#)]
10. Beck, S.E.; Ryu, H.; Boczek, L.A.; Cashdollar, J.L.; Jeanis, K.M.; Rosenblum, J.S.; Lawal, O.R.; Linden, K.G. Evaluating UV-C LED Disinfection Performance and Investigating Potential Dual-Wavelength Synergy. *Water Res.* **2017**, *109*, 207–216. [[CrossRef](#)]
11. Velten, S.; Hammes, F.; Boller, M.; Egli, T. Rapid and Direct Estimation of Active Biomass on Granular Activated Carbon through Adenosine Tri-Phosphate (ATP) Determination. *Water Res.* **2007**, *41*, 1973–1983. [[CrossRef](#)]
12. Acosta, N.; Bautista, M.A.; Hollman, J.; McCalder, J.; Beaudet, A.B.; Man, L.; Waddell, B.J.; Chen, J.; Li, C.; Kuzma, D.; et al. A Multicenter Study Investigating SARS-CoV-2 in Tertiary-Care Hospital Wastewater. Viral Burden Correlates with Increasing Hospitalized Cases as Well as Hospital-Associated Transmissions and Outbreaks. *Water Res.* **2021**, *201*, 117369. [[CrossRef](#)]
13. Bivins, A.; Greaves, J.; Fischer, R.; Yinda, K.C.; Ahmed, W.; Kitajima, M.; Munster, V.J.; Bibby, K. Persistence of SARS-CoV-2 in Water and Wastewater. *Environ. Sci. Technol. Lett.* **2020**, *7*, 937–942. [[CrossRef](#)]
14. Hamouda, M.; Mustafa, F.; Maraqa, M.; Rizvi, T.; Aly Hassan, A. Wastewater Surveillance for SARS-CoV-2: Lessons Learnt from Recent Studies to Define Future Applications. *Sci. Total Environ.* **2021**, *759*, 143493. [[CrossRef](#)]
15. Medema, G.; Heijnen, L.; Elsinga, G.; Italiaander, R.; Brouwer, A. Presence of SARS-Coronavirus-2 RNA in Sewage and Correlation with Reported COVID-19 Prevalence in the Early Stage of the Epidemic in The Netherlands. *Environ. Sci. Technol. Lett.* **2020**, *7*, 511–516. [[CrossRef](#)]
16. Meng, X.; Wang, X.; Meng, S.; Wang, Y.; Liu, H.; Liang, D.; Fan, W.; Min, H.; Huang, W.; Chen, A.; et al. A Global Overview of SARS-CoV-2 in Wastewater: Detection, Treatment, and Prevention. *ACS EST Water* **2021**, *1*, 2174–2185. [[CrossRef](#)]
17. Cerrada-Romero, C.; Berastegui-Cabrera, J.; Camacho-Martínez, P.; Goikoetxea-Aguirre, J.; Pérez-Palacios, P.; Santibáñez, S.; José Blanco-Vidal, M.; Valiente, A.; Alba, J.; Rodríguez-Álvarez, R.; et al. Excretion and Viability of SARS-CoV-2 in Feces and Its Association with the Clinical Outcome of COVID-19. *Sci. Rep.* **2022**, *12*, 7397. [[CrossRef](#)]
18. Cheung, K.S.; Hung, I.F.N.; Chan, P.P.Y.; Lung, K.C.; Tso, E.; Liu, R.; Ng, Y.Y.; Chu, M.Y.; Chung, T.W.H.; Tam, A.R.; et al. Gastrointestinal Manifestations of SARS-CoV-2 Infection and Virus Load in Fecal Samples from a Hong Kong Cohort: Systematic Review and Meta-Analysis. *Gastroenterology* **2020**, *159*, 81–95. [[CrossRef](#)]
19. Cuicchi, D.; Lazzarotto, T.; Poggioli, G. Fecal-Oral Transmission of SARS-CoV-2: Review of Laboratory-Confirmed Virus in Gastrointestinal System. *Int. J. Color. Dis.* **2021**, *36*, 437–444. [[CrossRef](#)]
20. Guo, M.; Tao, W.; Flavell, R.A.; Zhu, S. Potential Intestinal Infection and Faecal-Oral Transmission of SARS-CoV-2. *Nat. Rev. Gastroenterol. Hepatol.* **2021**, *18*, 269–283. [[CrossRef](#)]
21. Wang, W.; Xu, Y.; Gao, R.; Lu, R.; Han, K.; Wu, G.; Tan, W. Detection of SARS-CoV-2 in Different Types of Clinical Specimens. *JAMA* **2020**, *323*, 1843–1844. [[CrossRef](#)] [[PubMed](#)]
22. Rimoldi, S.G.; Stefani, F.; Gigantiello, A.; Polesello, S.; Comandatore, F.; Mileto, D.; Maresca, M.; Longobardi, C.; Mancon, A.; Romeri, F.; et al. Presence and Infectivity of SARS-CoV-2 Virus in Wastewaters and Rivers. *Sci. Total Environ.* **2020**, *744*, 140911. [[CrossRef](#)] [[PubMed](#)]
23. Inagaki, H.; Saito, A.; Sugiyama, H.; Okabayashi, T.; Fujimoto, S. Rapid Inactivation of SARS-CoV-2 with Deep-UV LED Irradiation. *Emerg. Microbes Infect.* **2020**, *9*, 1744–1747. [[CrossRef](#)] [[PubMed](#)]
24. Ruetalo, N.; Businger, R.; Schindler, M. Rapid, Dose-Dependent and Efficient Inactivation of Surface Dried SARS-CoV-2 by 254 nm UV-C Irradiation. *Eurosurveillance* **2021**, *26*, 2001718. [[CrossRef](#)] [[PubMed](#)]
25. Storm, N.; McKay, L.G.A.; Downs, S.N.; Johnson, R.I.; Birru, D.; de Samber, M.; Willaert, W.; Cennini, G.; Griffiths, A. Rapid and Complete Inactivation of SARS-CoV-2 by Ultraviolet-C Irradiation. *Sci. Rep.* **2020**, *10*, 22421. [[CrossRef](#)]
26. Bradford, M.M. A Rapid and Sensitive Method for the Quantitation of Microgram Quantities of Protein Utilizing the Principle of Protein-Dye Binding. *Anal. Biochem.* **1976**, *72*, 248–254. [[CrossRef](#)]

27. Whitney, O.N.; Kennedy, L.C.; Fan, V.B.; Hinkle, A.; Kantor, R.; Greenwald, H.; Crits-Christoph, A.; Al-Shayeb, B.; Chaplin, M.; Maurer, A.C.; et al. Sewage, Salt, Silica, and SARS-CoV-2 (4S): An Economical Kit-Free Method for Direct Capture of SARS-CoV-2 RNA from Wastewater. *Environ. Sci. Technol.* **2021**, *55*, 4880–4888. [[CrossRef](#)]
28. Yu, L.; Achari, G.; Langford, C.H. Design and Evaluation of a Novel Light-Emitting Diode Photocatalytic Reactor for Water Treatment. *J. Environ. Eng.* **2018**, *144*, 04018014. [[CrossRef](#)]
29. Yu, L.; Achari, G.; Langford, C.H. Design of a Homogeneous Radiation Field in an LED Photo-Reactor. *J. Environ. Eng. Sci.* **2014**, *9*, 214–223. [[CrossRef](#)]
30. Linklater, N.; Örmeci, B. Evaluation of the Adenosine Triphosphate (ATP) Bioluminescence Assay for Monitoring Effluent Quality and Disinfection Performance. *Water Qual. Res. J.* **2013**, *49*, 114–123. [[CrossRef](#)]
31. Yang, C.; Sun, W.; Ao, X. Bacterial Inactivation, DNA Damage, and Faster ATP Degradation Induced by Ultraviolet Disinfection. *Front. Environ. Sci. Eng.* **2019**, *14*, 13. [[CrossRef](#)]
32. Reardon, J.T.; Sancar, A. Nucleotide Excision Repair. *Prog. Nucleic Acid Res. Mol. Biol.* **2005**, *79*, 183–235.
33. Wang, Y.; Wang, Y.; Wang, Y.; Murray, C.K.; Hamblin, M.R.; Hooper, D.C.; Dai, T. Antimicrobial Blue Light Inactivation of Pathogenic Microbes: State of the Art. *Drug Resist. Updates* **2017**, *33–35*, 1–22. [[CrossRef](#)]
34. Nichia Inactivation Effect (99.99%) of Nichia’s Deep UV LEDs on the Novel Coronavirus (SARS-CoV-2). Available online: https://www.nichia.co.jp/en/newsroom/2020/2020_121701.html (accessed on 9 June 2022).
35. Biasin, M.; Bianco, A.; Pareschi, G.; Cavalleri, A.; Cavatorta, C.; Fenizia, C.; Galli, P.; Lessio, L.; Lualdi, M.; Tombetti, E.; et al. UV-C Irradiation Is Highly Effective in Inactivating SARS-CoV-2 Replication. *Sci. Rep.* **2021**, *11*, 6260. [[CrossRef](#)]
36. Robinson, C.A.; Hsieh, H.-Y.; Hsu, S.-Y.; Wang, Y.; Salcedo, B.T.; Belenchia, A.; Klutts, J.; Zemmer, S.; Reynolds, M.; Semkiw, E.; et al. Defining Biological and Biophysical Properties of SARS-CoV-2 Genetic Material in Wastewater. *Sci. Total Environ.* **2022**, *807*, 150786. [[CrossRef](#)]
37. Kim, S.; Kennedy, L.C.; Wolfe, M.K.; Criddle, C.S.; Duong, D.H.; Topol, A.; White, B.J.; Kantor, R.S.; Nelson, K.L.; Steele, J.A.; et al. SARS-CoV-2 RNA Is Enriched by Orders of Magnitude in Primary Settled Solids Relative to Liquid Wastewater at Publicly Owned Treatment Works. *Environ. Sci. Water Res. Technol.* **2022**, *8*, 757–770. [[CrossRef](#)]
38. Li, B.; Di, D.Y.W.; Saingam, P.; Jeon, M.K.; Yan, T. Fine-Scale Temporal Dynamics of SARS-CoV-2 RNA Abundance in Wastewater during a COVID-19 Lockdown. *Water Res.* **2021**, *197*, 117093. [[CrossRef](#)]
39. Huang, Y.; Yang, C.; Xu, X.; Xu, W.; Liu, S. Structural and Functional Properties of SARS-CoV-2 Spike Protein: Potential Antivirus Drug Development for COVID-19. *Acta Pharmacol. Sin.* **2020**, *41*, 1141–1149. [[CrossRef](#)]
40. Azzazy, E.; Christenson, R.H. *All about Albumin: Biochemistry, Genetics, and Medical Applications*; Peters, T., Jr., Ed.; Academic Press: San Diego, CA, USA, 1996; 432p, ISBN 0-12-552110-3.
41. Kerwin, B.A.; Remmele, R.L. Protect from Light: Photodegradation and Protein Biologics. *J. Pharm. Sci.* **2007**, *96*, 1468–1479. [[CrossRef](#)]
42. Silvester, J.A.; Timmins, G.S.; Davies, M.J. Photodynamically Generated Bovine Serum Albumin Radicals: Evidence for Damage Transfer and Oxidation at Cysteine and Tryptophan Residues. *Free Radic. Biol. Med.* **1998**, *24*, 754–766. [[CrossRef](#)]
43. Lo, C.-W.; Matsuura, R.; Iimura, K.; Wada, S.; Shinjo, A.; Benno, Y.; Nakagawa, M.; Takei, M.; Aida, Y. UVC Disinfects SARS-CoV-2 by Induction of Viral Genome Damage without Apparent Effects on Viral Morphology and Proteins. *Sci. Rep.* **2021**, *11*, 13804. [[CrossRef](#)] [[PubMed](#)]

Disclaimer/Publisher’s Note: The statements, opinions and data contained in all publications are solely those of the individual author(s) and contributor(s) and not of MDPI and/or the editor(s). MDPI and/or the editor(s) disclaim responsibility for any injury to people or property resulting from any ideas, methods, instructions or products referred to in the content.